



HAL
open science

Comparison of software accuracy to estimate the bed grain size distribution from digital images: A test performed along the Rhine River

Valentin Chardon, Guillaume Piasny, Laurent Schmitt

► **To cite this version:**

Valentin Chardon, Guillaume Piasny, Laurent Schmitt. Comparison of software accuracy to estimate the bed grain size distribution from digital images: A test performed along the Rhine River. *River Research and Applications*, 2022, 38 (2), pp.358 - 367. 10.1002/rra.3910 . hal-03634704

HAL Id: hal-03634704

<https://cnrs.hal.science/hal-03634704>

Submitted on 13 Apr 2022

HAL is a multi-disciplinary open access archive for the deposit and dissemination of scientific research documents, whether they are published or not. The documents may come from teaching and research institutions in France or abroad, or from public or private research centers.

L'archive ouverte pluridisciplinaire **HAL**, est destinée au dépôt et à la diffusion de documents scientifiques de niveau recherche, publiés ou non, émanant des établissements d'enseignement et de recherche français ou étrangers, des laboratoires publics ou privés.

Comparison of software accuracy to estimate the bed grain size distribution from digital images: A test performed along the Rhine River

Journal:	<i>River Research and Applications</i>
Manuscript ID	RRA-21-0183.R1
Wiley - Manuscript type:	Short Communication (Direct Via EEO)
Date Submitted by the Author:	28-Sep-2021
Complete List of Authors:	CHARDON, Valentin; CNRS, LIVE UMR 7362, Université de Strasbourg, 3 rue de l'Argonne, LIVE PIASNY, Guillaume; CNRS, LIVE UMR 7362, Université de Strasbourg, 3 rue de l'Argonne, LIVE Schmitt, Laurent; Université de Strasbourg, CNRS-ERL 7230 CNRS
Keywords:	bed grain size, digital images, software accuracy, river, Rhine

SCHOLARONE™
Manuscripts

1 **Comparison of software accuracy to estimate the bed grain size** 2 **distribution from digital images: A test performed along the Rhine River**

3 Valentin Chardon¹, Guillaume Piasny¹, Laurent Schmitt¹

4 1. CNRS UMR 7362 LIVE, University of Strasbourg, Strasbourg, France

5 Correspondence to: Valentin Chardon, CNRS UMR 7362 LIVE, University of Strasbourg, 3
6 rue de l'Argonne 67000 Strasbourg cedex, France.

7 E-mail: valentin.chardon@live-cnrs.unistra.fr

8 Telephone number: +33 3 68 85 09 76

9 **Abstract**

10 The quantification of the bed grain size distribution (GSD) of river surfaces is primarily
11 conducted through manual approaches in the field. These methods are time consuming
12 and not able to accurately represent the spatial diversity of the grain size distribution of
13 rivers. Recently, several software programmes and procedures have been developed
14 using semi-automatic and automatic methods to estimate bed GSD from digital imagery.
15 The purpose of this study is to compare softwares accuracy between reference GSDs and
16 estimated GSDs using geometric approaches (Basegrain software and a procedure
17 developed on ImageJ), statistical approaches (Digital Grain Size (DGS) and PebbleCounts
18 softwares) and a machine learning framework (SediNet). This study evaluates ten digital
19 images recorded along the Rhine River downstream of the city of Basel. The results
20 showed that all software programmes considerably underestimated the manually
21 measured GSDs. Nevertheless, it is possible to significantly improve the estimation of bed
22 GSD by applying calibration laws. Both DGS and Basegrain softwares are reliable to
23 estimate the GSD, while the three others softwares are accurate for percentiles equal and

1
2 24 higher than the D_{50} . After linear regression correction, the mean NRMSE of percentile
3
4 25 errors did not exceed 13% for DGS and Basegrain software, while the others not exceed
5
6 26 22% for percentiles coarser than the D_{50} .
7
8
9

10 27 **Key words:** bed grain size, digital images, software accuracy, river, Rhine
11
12

13 28 1. Introduction

14
15
16 29 Riverbed grain size is a key parameter in geomorphological and ecological studies of
17 30 rivers. This parameter allows researchers to evaluate physical habitat quality, sediment
18 31 transport dynamics and restoration action effects. The quantification of the bed grain size
19 32 distribution (GSD) of river surfaces is mostly conducted through manual approaches in the
20 33 field, such as Wolman sampling, the paint-and-pick approach or grid sampling (Bunte &
21 34 Abt, 2001). These methods are time consuming and obtained punctual measurements are
22 35 not representative of the spatial diversity of a river's grain size distribution (Graham et al.,
23 36 2010). Currently, new remote sensing methods have been developed to semi-
24 37 automatically or automatically estimate the bed GSD of bar surfaces. These approaches
25 38 are divided into two classes: (i) two-dimensional approaches using terrestrial and aerial
26 39 imagery (Baptista et al., 2012; Chang & Chung, 2012; Chardon et al., 2021; Graham et al.,
27 40 2005; Lejot et al., 2011; Purinton & Bookhagen, 2019; Rubin, 2004; Strom et al., 2010;
28 41 Sulaiman et al., 2014; Turley et al., 2017) and (ii) three-dimensional approaches using
29 42 photogrammetry, laser scanning or LiDAR datasets by estimating roughness as a proxy of
30 43 bed GSD (Brasington et al., 2012; Chardon et al., 2020; Heritage & Milan, 2009; Vázquez-
31 44 Tarrío et al., 2017; Woodget et al., 2018). Although the photographic sampling method
32 45 does not enable the mapping of surface GSD over a large area as usually with a three-
33 46 dimensional approach, it requires only a simple camera and thus is less costly than the
34 47 precendently mentionned. Moreover, terrestrial photographic sampling requires fewer
35 48 preprocessing steps for correcting raw data than three-dimensional approaches, which can

1
2 49 be difficult and technical (e.g., cleaning and georeferencing of raw point clouds, roughness
3
4 50 metric calculation and calibration with the manual field GSD) (Brasington et al., 2012;
5
6 51 Heritage & Milan, 2009; Vázquez-Tarrío et al., 2017; Woodget et al., 2018). However, the
7
8 52 accuracy of two-dimensional approaches is extremely sensitive to environmental
9
10
11 53 conditions such as sun illumination, the presence of vegetation or biofilms, and sediment
12
13 54 petrography or/and mineralogy. In addition, for suhtwo-dimensional approaches, bed
14
15 55 sediment structures (burial, overlapping and foreshortening) also influence the accuracy of
16
17 56 the obtained results (Graham et al., 2010; Hodge et al., 2009).

18
19
20 57 Two methods were used to estimate the bed GSD from digital images via morphological
21
22 58 approaches and statistical approaches (Buscombe, 2013). Morphological approaches use
23
24 59 thresholding and segmentation processing to define the outline of each visible particle,
25
26 60 while statistical approaches tend to estimate the grain size through image texture analysis
27
28 61 from the semi-variance approach (Carbonneau et al., 2004), autocorrelation approach
29
30 62 (Warrick et al., 2009), the wavelength approach (Buscombe, 2013) and recently following
31
32 63 the k-means approach (Puriton et al., 2019). Deep learning methods were also developed
33
34 64 to estimate automatically the GSD using digital images as SediNet (Buscombe, 2020) and
35
36 65 GRAINet (Lang et al., 2021). Although Basegrain (morphological approach) and DGS
37
38 66 (statistical approach) programs are frequently used to estimate the GSD from digital
39
40 67 images, a question still remains: which software provides, using default parameters, the
41
42 68 most accurate estimation of bed GSD from digital imagery? The objective of this study is to
43
44 69 compare the software accuracy of reference GSDs and estimated GSDs from DGS,
45
46 70 Basegrain, SediNet, PebbleCounts software and a procedure using ImageJ. The analysis
47
48 71 was based on ten digital images sampled along the Rhine River downstream of the city of
49
50 72 Basel.

51 73 **2. Methodology**

74 2.1 Study area

75 Photographic sampling was performed on the Old Rhine River between the cities of
76 Kembs and Ottmarsheim over five above-water deposits. The Old Rhine River is a
77 bypassed and regulated reach in the Alsacian Plain. An instream flow is maintained in the
78 Old Rhine between 52 and 115 m³/s from the Kembs derivation dam, depending on the
79 natural hydrological regime of the Rhine River (Fig. 1b). Spills occur in the Old Rhine River
80 when the Rhine River discharge exceeds 1400 m³/s in Basel, which is the maximum flow
81 capacity discharge of the Grand Canal d'Alsace (GCA). The channel bottom of the study
82 reach is composed mainly of gravel and cobble (Arnaud et al., 2015). The mean slope and
83 mean width are equal to 0.09% and 100m, respectively (Fig. 1b).

84 2.2 Field data collection

85 Photographic sampling was performed on clean substrates without vegetation or a biofilm
86 to avoid substantial estimation errors induced by these elements (Chardon et al. 2020).
87 According to the recommendations of Barnard et al. (2007) and Chardon et al. (2020), all
88 digital images were taken under an umbrella in order to control solar conditions which
89 could influence GSD estimations (Fig. 1). Moreover, all images were taken using a
90 telescoping bar and a bubble level to capture sediment patches with a horizontal plane of
91 view. The camera used was an Olympus TG-4, and the image resolution was equal to 16
92 MP (4608 x 3456 pixel). A median filter was applied to reduce error in the estimation
93 resulting from pepper and salt phenomena (Chardon et al., 2020). As recommended by
94 Chardon et al. (2020), the median-sized filter used in this study was equal to 5% of the
95 Dmax value measured for each digital image.

96 2.3 Image processing

97 2.3.1 Manual digitalization

1
2 98 Following the recommendations of Barnard et al. (2007), the b-axes of 80 to 100 particles
3
4 99 were digitized manually from each digital image using a sampling grid to obtain a
5
6 100 reference distribution. This step, which was performed using ImageJ software, allows us to
7
8
9 101 achieve a reference GSD.

10 11 12 102 2.3.2 DGS software

13
14
15 103 The first software used to automatically estimate the grain size of 10 sediment patches
16
17 104 was the DGS software developed by Buscombe and implemented in MATLAB (2013). This
18
19 105 software is based on a statistical approach using the wavelength method which
20
21 106 automatically provides the GSD in grid sampling (Fig. 2). . Batch processing has been
22
23
24 107 proposed to evaluate the GSD of a large number of digital images. No filter was applied,
25
26 108 and the totality of the surfaces of the digital images was considered for GSD estimation.

27 28 29 30 109 2.3.3 Basegrain software

31
32
33 110 The second software used in this study is Basegrain software (Detert and Weitbrecht,
34
35 111 2013), which was also developed for MATLAB software (Fig. 3). The approach of
36
37 112 Basegrain is based on a morphological method. Five preprocessing steps are available for
38
39 113 the user to compute median filter options, the minimal size of a grain area (for watershed
40
41 114 algorithm application) and the minimal number of pixels (to determine the minimal area),
42
43 115 which is related to grain size (Detert and Weitbrecht, 2013). This study used the default
44
45 116 options for each step to decrease the processing time of digital images and to compare the
46
47 117 methods between them without to not to favour one method over another. The GSD can
48
49 118 be obtained in a grid sampling form.

50 51 52 53 54 119 2.3.4 Procedure using ImageJ software

55
56
57 120 The method using ImageJ is based on a procedure established by (Sulaiman et al., 2014),
58
59 121 which proposed a morphological approach to automatically extract the GSD by areal

1
2 122 sampling. We slightly changed this protocol as follows: (i) the digital images are
3
4 123 transformed in 8-bit format, (ii) the substrate background algorithm is applied with mobile
5
6 124 windows equal to 50 pixels by default, (iii) an automatic threshold for black and white
7
8
9 125 transformation is applied, (iv) the watershed algorithm is applied and (v) the b-axis of all
10
11 126 detected particles were determined via automatic measurement (Fig. 5). To compare the
12
13 127 GSD obtained with this method (areal sampling) to the two previous estimations from DGS
14
15
16 128 and Basegrain software, we collected the b-axis of 60 to 100 particles detected using a
17
18 129 grid built with QGIS software.

21 130 2.3.5 PebbleCounts software

22
23
24 131 This software was developed in Python language and used initially to estimate the
25
26
27 132 apparent GSD of above-water bar deposits using aerial imagery from a drone (Puriton &
28
29 133 Bookhagen., 2019). This software was recently used to estimate the longitudinal bed grain
30
31 134 size variations along 100 km of river length of the Toro watershed located in Argentina
32
33
34 135 (Puriton & Bookhagen, 2021). In this study, we used the automatic procedure named as
35
36 136 PebbleCountsAuto (AIF) which used edge detection and filter automatically suspect grains
37
38 137 (Puriton & Bookhagen., 2019). Same as the procedure in ImageJ software, we collected
39
40 138 the b-axis of 60 to 100 particles detected using a grid built with QGIS software from X and
41
42
43 139 Y coordinates provided by the output files of the software.

46 140 2.3.6 SediNet software

47
48
49 141 This software was based on machine learning framework developed by Buscombe (2019)
50
51
52 142 using python language. It allows to estimate quantitatively and automatically the
53
54 143 measurements from digital images and given percentiles values directly at the output. In
55
56 144 this study, we used the trainer developed only for gravel deposits related to our dataset.

59 145 2.4 Estimation of the prediction accuracy

1
2 146 To evaluate and compare the prediction accuracy of each software, we compared
3
4 147 percentile values estimated by each automatic processing to the reference distributions.
5
6 148 The variation between the predicted and reference values was quantified by two metrics,
7
8
9 149 i.e., the NRMSE (Eq. 1) and NMAE (Eq. 2), which were calculated as follows:

$$10$$

$$11$$

$$12$$

$$13$$

$$14$$

$$15$$

$$16$$

$$17$$

$$18$$

$$19$$

$$20$$

$$21$$

$$22$$

$$23$$

$$24$$

$$25$$

$$26$$

$$27$$

$$28$$

$$29$$

$$30$$

$$31$$

$$32$$

$$33$$

$$34$$

$$35$$

$$36$$

$$37$$

$$38$$

$$39$$

$$40$$

$$41$$

$$42$$

$$43$$

$$44$$

$$45$$

$$46$$

$$47$$

$$48$$

$$49$$

$$50$$

$$51$$

$$52$$

$$53$$

$$54$$

$$55$$

$$56$$

$$57$$

$$58$$

$$59$$

$$60$$

$$NRMSE = \frac{\sqrt{\sum_{i=1}^n (x_i - x)^2}}{x_{mean}} \quad (1)$$

$$NMAE = \frac{\left(\frac{\sum_{i=1}^n |(x_i - x)|}{n} \right)}{x_{mean}} \quad (2)$$

152 where x_i is equal to the value of the predicted percentile and x is the value of the manually
153 measured percentile. x_{mean} corresponds to the mean value of the percentile manually
154 measured for the digital image dataset.

155 3. Results

156 3.1 Software accuracy before calibration

157 Fig. 6 shows that all softwares underestimated all percentiles. The results are quite similar
158 for Basegrain software from D_{10} to D_{50} , with a net underestimation of these percentiles
159 (Tab. 1). In contrast, from D_{75} to D_{95} , an overestimation occurred using Basegrain (Tab. 1).
160 Globally, for all software programmes, the NRMSE and NMAE decrease according to the
161 increase in the estimated percentile (Fig. 7). However, the values of these parameters
162 differ considerably between the compared software programmes. For DGS software, the
163 maximal NRMSE and NMAE values of percentile errors were equal to 56% and 47%,
164 respectively. For Basegrain software, the maximal NRMSE and NMAE values were equal
165 to 97% and 90%, respectively (Fig. 7). For the ImageJ procedure, the maximal RMSE and

1
2 166 NMAE values equal 88% and 79%, respectively. For SediNet, the maximal RMSE and
3
4 167 NMAE values equal 67% and 58%, respectively. For PebbleCounts, the maximal RMSE
5
6 168 and NMAE values equal 71% and 59%, respectively.
7
8
9

10 169 3.2 Software accuracy after calibration

11
12
13 170 Significant linear relationships were found between the manually measured and predicted
14
15 171 percentiles by DGS and Basegrain software (Tab. 1.) Only significant statistical linear
16
17 172 relationships were found from D_{75} between the predicted and manually measured
18
19 173 percentiles by the procedure using ImageJ software (Tab. 1). For SediNet, significant
20
21 174 statistical relationships were found for D_{10} , D_{16} , D_{25} , and D_{84} , respectively. Whereas for
22
23 175 PebbleCounts, significant relations were found from the D_{75} (Tab. 1). For the latest, no
24
25 176 relationship was observed for the D_{10} with a R-square close to 0.
26
27
28
29

30 177 Through the application of linear regressions, a reduction in NRMSE and NMAE occurred
31
32 178 for all percentiles and all procedures between the corrected-predicted percentiles and
33
34 179 manually measured percentile due to a high reduction of the previous under-estimation of
35
36 180 before correction (Fig. 7; Fig. 8). For DGS software, the maximal NRMSE and NMAE
37
38 181 values of percentile errors were equal to 20% and 17%, respectively. For Basegrain
39
40 182 software, the maximal RMSE and NMAE values of the percentile errors were equal to 20%
41
42 183 and 16%, respectively. For the ImageJ procedure, the maximal RMSE and NMAE values
43
44 184 were equal to 40% and 33%, respectively (Fig. 7). For SediNet, the maximal RMSE and
45
46 185 NMAE values were equal to 33% and 23%, respectively. Finally, for PebbleCounts, the
47
48 186 maximal RMSE and NMAE values were equal to 38% and 33% excluding the D_{10} .
49
50
51
52

53
54 187

55
56
57 188

58
59
60 189

4. Discussion

4.1 Comparison of software accuracy

Our results showed that all methods underestimated the GSD with great error in comparison to the reference GSD obtained through the manual approach. This underestimation is explained by an oversegmentation of particles due to petrographic variation (Sime & Ferguson, 2003; Strom et al., 2010; Warrick et al., 2009). To reduce the error estimations, a calibration correction must be applied to improve the GSD estimation, as that proposed by Chardon et al. (2020) (Fig. 7; Fig. 8). Our results show that both DGS and Basegrain are reliable software programmes to estimate the GSD on digital images after linear regression correction (Fig. 8). The maximal value of error estimation was less than 18% (NMAE) after the linear correction (Fig. 7). The other three softwares are also reliable for percentiles estimation coarser than the D_{50} (Fig. 7). The maximal value of error estimation was equal to 22% (NMAE for SediNet) after linear correction (Fig. 7).

4.2 Software advantages and limitations

Each software presents advantages and limitations. For DGS software, the GSD was obtained quickly, and no extra preprocessing step than a median filter application was necessary. Nevertheless, this software is similar to a “black box” with no means to see the detected particles and perform error localization in digital images, which does not allow to evaluate which parameter primarily influences the particle detection. This means that there is no possible way to change the software parameters. The same limitation occurs for SediNet due to the deep learning method used. For PebbleCounts software, the advantage is that only one parameter required from the user before computation and the results of the grain identification are visible in a new window. On the other hand, Basegrain software allows you to view the detected particles and spatial errors but also allows operator intervention to modify or delete the detected particle outlines. However, in some

1
2 215 cases, numerous visual checks may be necessary during the preprocessing steps (n=5) to
3
4 216 obtain satisfying results. In our cases, to be consistent with the idea of quick and easy data
5
6 217 processing, no calibration steps were implemented, and the GSD being estimated by the
7
8 218 automatic object detection tool of Basegrain. For the ImageJ procedure, the main limitation
9
10 219 is the application of step 3, which consists of applying an automatic threshold for black and
11
12 220 white transformation that is necessary for the application of the watershed algorithm.
13
14 221 Because pixel color values differ between each digital image, it is very difficult to find a
15
16 222 single threshold for a set of digital images. In addition the several manual preprocessing
17
18 223 steps of this procedure increase the processing time (Fig.5), which may be problematic for
19
20 224 large datasets.
21
22
23
24
25

26 225 4.3 Future research avenues

27
28
29 226 The main advantage of using terrestrial digital images rather than aerial images or three-
30
31 227 dimensional techniques (photogrammetric or LiDAR data) is the low required material cost.
32
33 228 It is also a less time-consuming post-processing approach as most of the measurement
34
35 229 errors could be avoided during the field data collection (vegetation, biofilm, sun, etc.), and
36
37 230 less specific technical knowledge than three-dimensional approaches are needed. Thus,
38
39 231 this method could be easily used by river managers to quickly estimate the bed GSD on
40
41 232 both clean above and underwater bars for the planning step of river restoration projects,
42
43 233 evaluate natural changes or integrate bed GSD spatial distribution in numerical
44
45 234 hydrosedimentary models. However, questions still remain: what is the best sampling
46
47 235 procedure to integrate the spatio-temporal variability of the GSD? Because digital images
48
49 236 allows to estimate the local bed grain size quickly, how to estimate the GSD from this
50
51 237 sampling procedure at a larger spatial scale, similar to aerial or three-dimensional
52
53 238 approaches? Is this approach is a compromise between quantity and quality? More
54
55 239 studies have to be conducted in this topic to determine a robust sampling protocol using
56
57 240 digital images. Each of these sampling protocols should be guided by (i) the main objective
58
59
60

1
2 241 of the study, (ii) the sampling effort and (iii) the precision, which must be consistent with
3
4 242 the final use of the data.
5
6

7 243 **5. Conclusion**

8
9
10
11 244 The purpose of this study was to evaluate and compare the accuracy of GSD estimations
12
13 245 from ten digital images recorded on the Rhine River using five software programmes.
14
15 246 Results showed that all software programmes underestimated manually measured GSDs.
16
17 247 However, after linear regression correction, the NMAE decreased and did not exceed 18%
18
19 248 for the DGS and Basegrain software for all percentiles. For the three other softwares, the
20
21 249 estimation is reliable for percentiles higher than the D_{50} with a NMAE below 22%. This
22
23 250 study shows that it is possible to estimate the bed GSD of clean substrates in a precise
24
25 251 manner using DGS and Basegrain softwares for the entire distribution and the three other
26
27 252 softwares for percentiles equal and higher than the D_{50} . However, a calibration step must
28
29
30
31 253 be applied in all cases.
32
33
34

35 254 **ACKNOWLEDGMENTS**

36
37
38 255 None
39
40
41

42 256
43

44 257 **Conflict of Interest**

45
46
47 258 None
48
49
50

51 259
52
53

54 260
55
56

57 261
58
59

60 262

1
2 2633
4
5 264
6
78
9 265 **REFERENCES**

10
11
12 266 Arnaud, F., Piégay, H., Schmitt, L., Rollet, A. J., Ferrier, V., & Béal, D. (2015). Historical
13
14 267 geomorphic analysis (1932–2011) of a by-passed river reach in process-based
15
16 restoration perspectives: The Old Rhine downstream of the Kembs diversion dam
17 268 (France, Germany). *Geomorphology*, 236, 163–177.

18
19 269
20
21 270 <https://doi.org/10.1016/j.geomorph.2015.02.009>

22
23
24
25 271 Baptista, P., Cunha, T. R., Gama, C., & Bernardes, C. (2012). A new and practical method
26
27 272 to obtain grain size measurements in sandy shores based on digital image
28
29 273 acquisition and processing. *Sedimentary Geology*, 282, 294–306.

30
31 274 <https://doi.org/10.1016/j.sedgeo.2012.10.005>

32
33
34
35 275 Barnard, P. L., Rubin, D. M., Harney, J., & Mustain, N. (2007). Field test comparison of an
36
37 276 autocorrelation technique for determining grain size using a digital ‘beachball’
38
39 277 camera versus traditional methods. *Sedimentary Geology*, 201(1–2), 180–195.

40
41 278 <https://doi.org/10.1016/j.sedgeo.2007.05.016>

42
43
44
45 279 Brasington, J., Vericat, D., & Rychkov, I. (2012). Modeling river bed morphology,
46
47 280 roughness, and surface sedimentology using high resolution terrestrial laser
48
49 281 scanning: MODELING RIVER BED MORPHOLOGY WITH TLS. *Water Resources*

50
51 282 *Research*, 48(11). <https://doi.org/10.1029/2012WR012223>

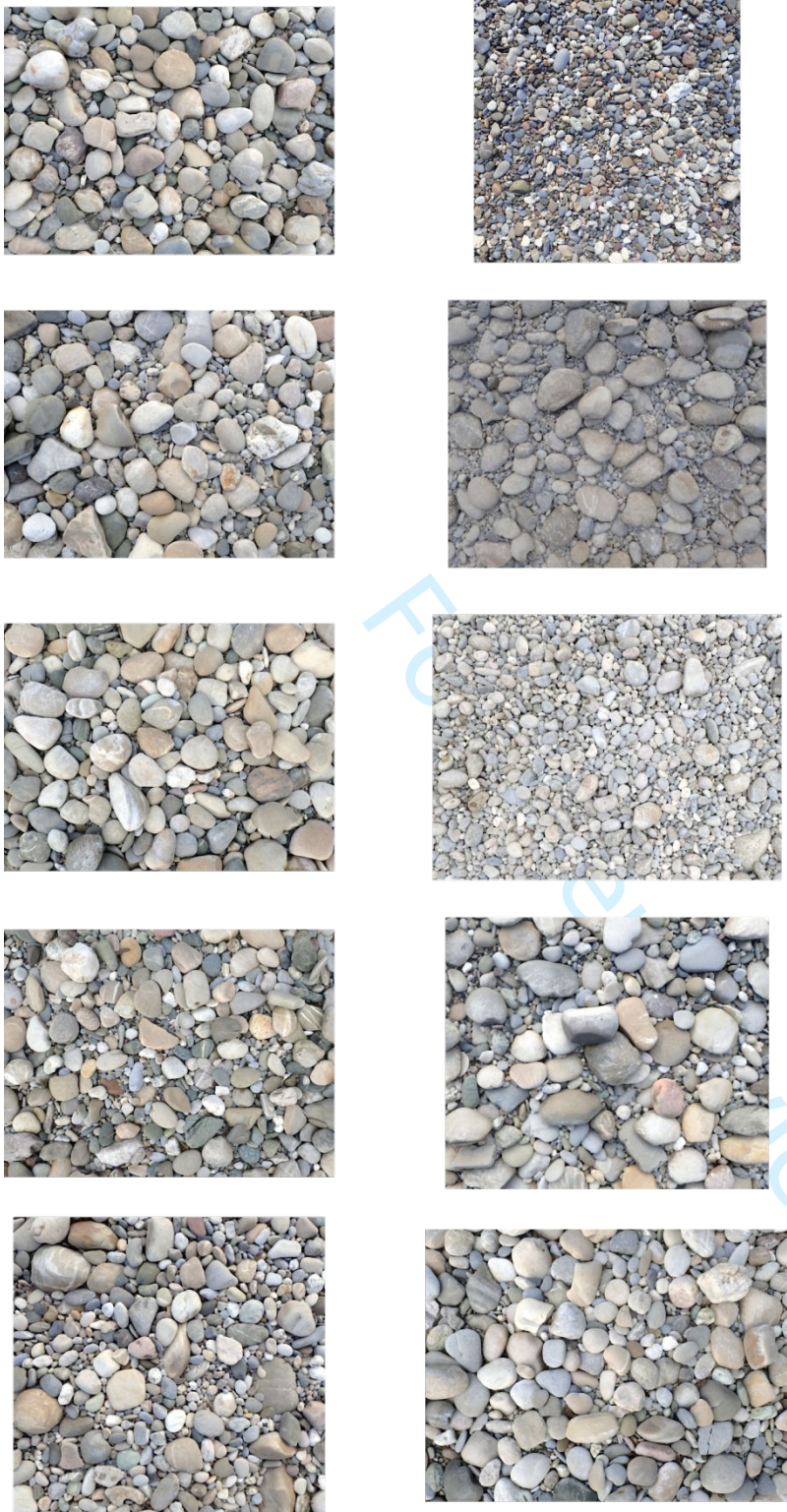
52
53
54
55 283 Bunte, K., & Abt, S. R. (2001). *Sampling surface and subsurface particle-size distributions*
56
57 284 *in wadable gravel-and cobble-bed streams for analyses in sediment transport,*
58
59 285 *hydraulics, and streambed monitoring* (RMRS-GTR-74; p. RMRS-GTR-74). U.S.

- 1
2 286 Department of Agriculture, Forest Service, Rocky Mountain Research Station.
3
4 287 <https://doi.org/10.2737/RMRS-GTR-74>
5
6
7
8 288 Buscombe, D., Rubin, D. M., & Warrick, J. A. (2010). A universal approximation of grain
9
10 289 size from images of noncohesive sediment: GRAIN SIZE FROM IMAGES OF
11
12 290 SEDIMENT. *Journal of Geophysical Research: Earth Surface*, 115(F2).
13
14 291 <https://doi.org/10.1029/2009JF001477>
15
16
17
18 292 Buscombe, Daniel. (2013). Transferable wavelet method for grain-size distribution from
19
20 293 images of sediment surfaces and thin sections, and other natural granular patterns.
21
22 294 *Sedimentology*, 60(7), 1709–1732. <https://doi.org/10.1111/sed.12049>
23
24
25
26 295 Buscombe, D. (2019). SediNet: a configurable deep learning model for mixed qualitative
27
28 296 and quantitative optical granulometry. *Earth Surface Processes and Landforms* 45
29
30 297 (3), 638-651. <https://onlinelibrary.wiley.com/doi/abs/10.1002/esp.4760>
31
32
33
34 298 Carbonneau, P. E., Lane, S. N., & Bergeron, N. E. (2004). Catchment-scale mapping of
35
36 299 surface grain size in gravel bed rivers using airborne digital imagery: MAPPING
37
38 300 GRAIN SIZE IN GRAVEL BED RIVERS. *Water Resources Research*, 40(7).
39
40 301 <https://doi.org/10.1029/2003WR002759>
41
42
43
44 302 Chang, F.-J., & Chung, C.-H. (2012). Estimation of riverbed grain-size distribution using
45
46 303 image-processing techniques. *Journal of Hydrology*, 440–441, 102–112.
47
48 304 <https://doi.org/10.1016/j.jhydrol.2012.03.032>
49
50
51
52 305 Chardon, V., Schmitt, L., Arnaud, F., Piégay, H., & Clutier, A. (2021). Efficiency and
53
54 306 sustainability of gravel augmentation to restore large regulated rivers: Insights from
55
56 307 three experiments on the Rhine River (France/Germany). *Geomorphology*, 380,
57
58 308 107639. <https://doi.org/10.1016/j.geomorph.2021.107639>
59
60

- 1
2 309 Chardon, V., Schmitt, L., Piégay, H., & Lague, D. (2020). Use of terrestrial photosieving
3
4 310 and airborne topographic LiDAR to assess bed grain size in large rivers: A study on
5
6 311 the Rhine River. *Earth Surface Processes and Landforms*, 45(10), 2314–2330.
7
8
9 312 <https://doi.org/10.1002/esp.4882>
10
11
12 313 Detert, M., Weitbrecht, V. (2012). Automatic object detection to analyze the geometry of
13
14 314 gravel grains – a free stand-alone tool. *River Flow 2012*, R.M. Muños (Ed.), Taylor
15
16 315 & Francis Group, London, ISBN 978-0-415-62129-8, pp. 595-600.
17
18
19
20 316 Graham, D. J., Reid, I., & Rice, S. P. (2005). Automated Sizing of Coarse-Grained
21
22 317 Sediments: Image-Processing Procedures. *Mathematical Geology*, 37(1), 1–28.
23
24 318 <https://doi.org/10.1007/s11004-005-8745-x>
25
26
27
28 319 Graham, D. J., Rollet, A. J., Piégay, H., & Rice, S. P. (2010). Maximizing the accuracy of
29
30 320 image-based surface sediment sampling techniques. *Water Resources Research*,
31
32 321 46(2), 1–15. <https://doi.org/10.1029/2008WR006940>
33
34
35
36 322 Heritage, G. L., & Milan, D. J. (2009). Terrestrial Laser Scanning of grain roughness in a
37
38 323 gravel-bed river. *Geomorphology*, 113(1–2), 4–11.
39
40 324 <https://doi.org/10.1016/j.geomorph.2009.03.021>
41
42
43
44 325 Hodge, R., Brasington, J., & Richards, K. (2009). Analysing laser-scanned digital terrain
45
46 326 models of gravel bed surfaces: Linking morphology to sediment transport processes
47
48 327 and hydraulics. *Sedimentology*, 56(7), 2024–2043. [https://doi.org/10.1111/j.1365-](https://doi.org/10.1111/j.1365-3091.2009.01068.x)
49
50 328 [3091.2009.01068.x](https://doi.org/10.1111/j.1365-3091.2009.01068.x)
51
52
53
54 329 Lang, N., Irniger, A., Rozniak, A., Hunziker, R., Wegner, J. D., and Schindler, K., (2021).
55
56 330 GRAINet: mapping grain size distributions in river beds from UAV images with
57
58 331 convolutional neural networks, *Hydrol. Earth Syst. Sci.*, 25, 2567–2597.
59
60 332 <https://doi.org/10.5194/hess-25-2567-2021>, 2021.

- 1
2 333 Lejot, J., Piégay, H., Hunter, P. David., Moulin, B., & Gagnage, M. (2011). Utilisation de la
3
4 334 télédétection pour la caractérisation des corridors fluviaux: Exemples d'applications
5
6 335 et enjeux actuels. *Géomorphologie : relief, processus, environnement*, 17(2), 157–
7
8 336 172. <https://doi.org/10.4000/geomorphologie.9362>
9
10
11
12 337 Purinton, B., & Bookhagen, B. (2019). Introducing PebbleCounts: A grain-sizing tool for
13
14 338 photo surveys of dynamic gravel-bed rivers. *Earth Surface Dynamics*, 7(3), 859–
15
16 339 877. <https://doi.org/10.5194/esurf-7-859-2019>
17
18
19
20 340 Purinton, B., & Bookhagen, B. (2021). Tracking downstream variability in large grain-size
21
22 341 distributions in the south-central Andes. *Journal of Geophysical Research: Earth*
23
24 342 *Surface*, 126, e2021JF006260. <https://doi.org/10.1029/2021JF006260>
25
26
27
28 343 Rubin, D. M. (2004). A Simple Autocorrelation Algorithm for Determining Grain Size from
29
30 344 Digital Images of Sediment. *Journal of Sedimentary Research*, 74(1), 160–165.
31
32 345 <https://doi.org/10.1306/052203740160>
33
34
35
36 346 Sime, L. C., & Ferguson, R. I. (2003). Information on Grain Sizes in Gravel-Bed Rivers by
37
38 347 Automated Image Analysis. *Journal of Sedimentary Research*, 73(4), 630–636.
39
40 348 <https://doi.org/10.1306/112102730630>
41
42
43
44 349 Strom, K. B., Kuhns, R. D., & Lucas, H. J. (2010). Comparison of Automated Image-Based
45
46 350 Grain Sizing to Standard Pebble-Count Methods. *Journal of Hydraulic Engineering*,
47
48 351 136(8), 461–473. [https://doi.org/10.1061/\(ASCE\)HY.1943-7900.0000198](https://doi.org/10.1061/(ASCE)HY.1943-7900.0000198)
49
50
51
52 352 Sulaiman, M. S., Sinnakaudan, S. K., Ng, S. F., & Strom, K. (2014). Application of
53
54 353 automated grain sizing technique (AGS) for bed load samples at Rasil River: A case
55
56 354 study for supply limited channel. *CATENA*, 121, 330–343.
57
58 355 <https://doi.org/10.1016/j.catena.2014.05.013>
59
60

- 1
2 356 Turley, M. D., Bilotta, G. S., Arbocuite, G., Chadd, R. P., Extence, C. A., & Brazier, R. E.
3
4 357 (2017). Quantifying Submerged Deposited Fine Sediments in Rivers and Streams
5
6 358 Using Digital Image Analysis: Quantifying fine sediment in rivers and streams using
7
8 359 DIA. *River Research and Applications*, 33(10), 1585–1595.
9
10 <https://doi.org/10.1002/rra.3073>
11 360
12
13
14 361 Vázquez-Tarrío, D., Borgniet, L., Liébault, F., & Recking, A. (2017). Using UAS optical
15
16 362 imagery and SfM photogrammetry to characterize the surface grain size of gravel
17
18 363 bars in a braided river (Vénéon River, French Alps). *Geomorphology*, 285, 94–105.
19
20 <https://doi.org/10.1016/j.geomorph.2017.01.039>
21 364
22
23
24 365 Warrick, J. A., Rubin, D. M., Ruggiero, P., Harney, J. N., Draut, A. E., & Buscombe, D.
25
26 366 (2009). Cobble cam: Grain-size measurements of sand to boulder from digital
27
28 367 photographs and autocorrelation analyses. *Earth Surface Processes and*
29
30 368 *Landforms*, 34(13), 1811–1821. <https://doi.org/10.1002/esp.1877>
31
32
33
34 369 Woodget, A. S., Fyffe, C., & Carbonneau, P. E. (2018). From manned to unmanned
35
36 370 aircraft: Adapting airborne particle size mapping methodologies to the
37
38 371 characteristics of sUAS and SfM. *Earth Surface Processes and Landforms*, 43(4),
39
40 372 857–870. <https://doi.org/10.1002/esp.4285>
41
42
43
44
45 373
46
47
48 374
49 375
50 376
51
52
53
54
55
56
57
58
59
60



378 Fig. 1: Set of sediments deposits studied (n=10). A median filter was applied before
379 analysis following the recommendations of Chardon et al., (2020).

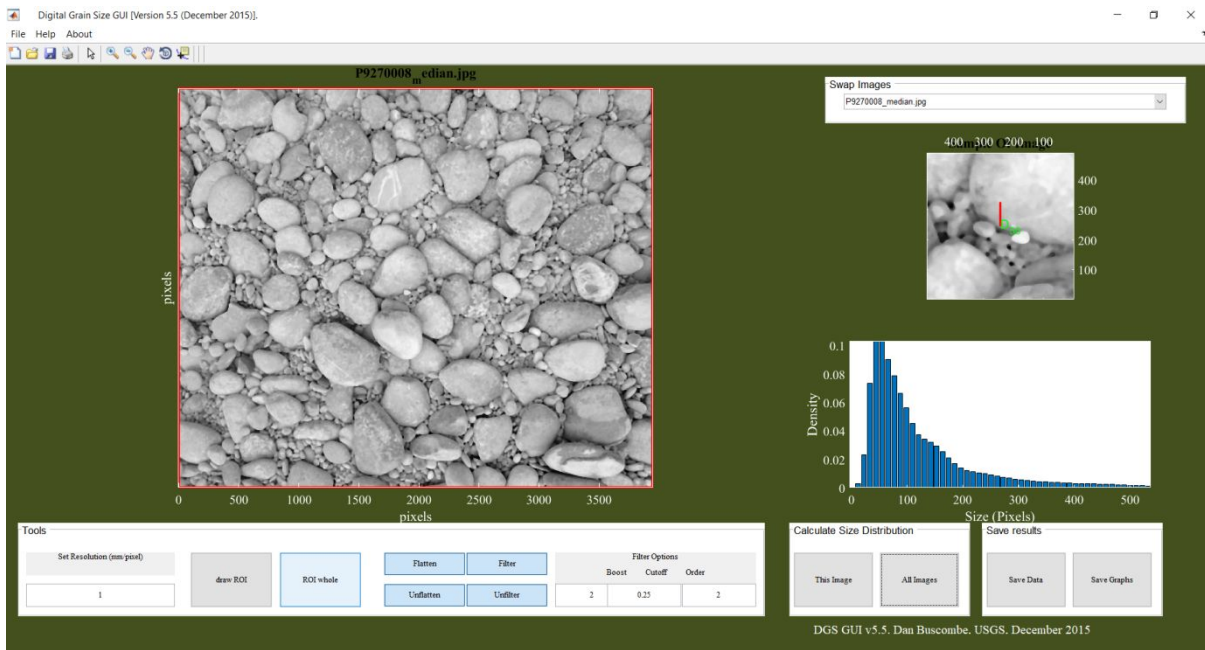
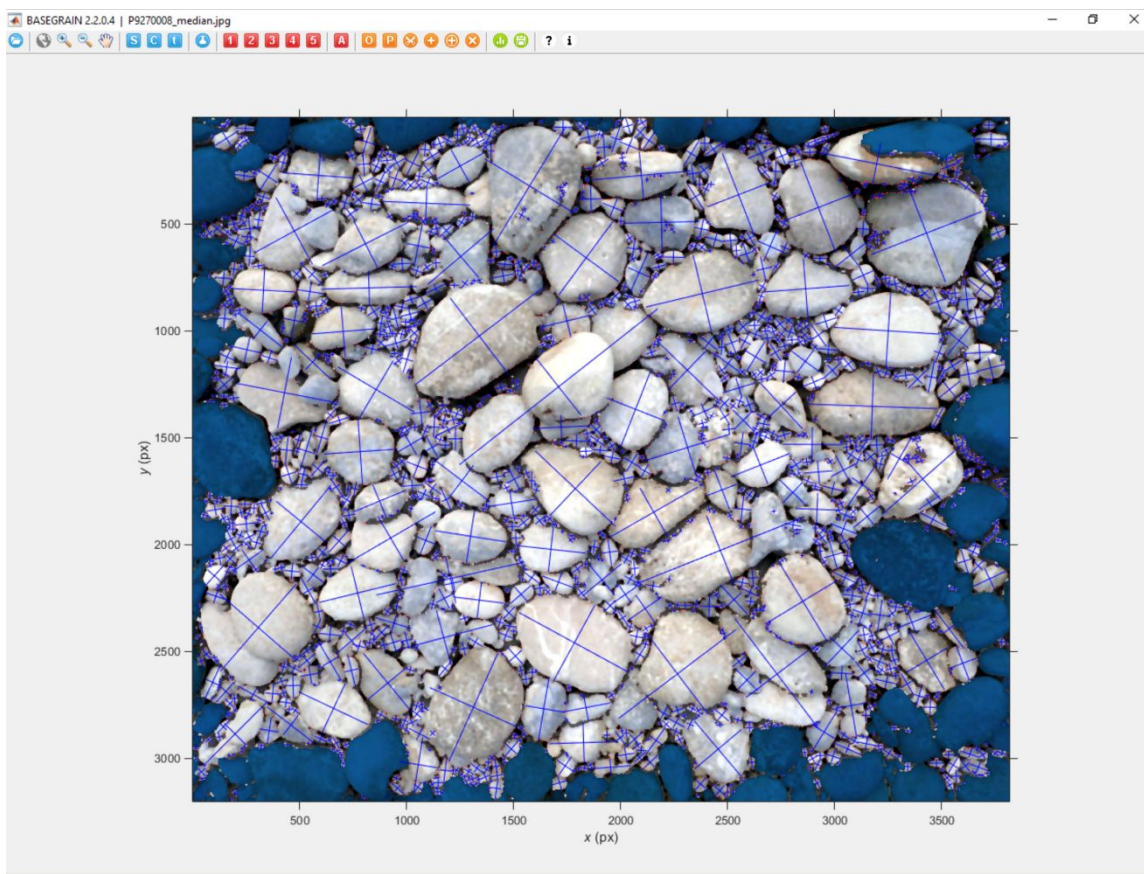


Fig. 2: Example of image processing by DGS software developed by Buscombe (2013).

1
2
3
4
5
6
7
8
9
10
11
12
13
14
15
16
17
18
19
20
21
22
23
24
25
26
27
28
29
30
31
32
33
34
35
36
37
38
39
40
41
42
43
44
45
46
47
48
49
50
51
52
53
54
55
56
57
58
59
60



391

392 Fig. 3: Example of image processing by Basegrain software developed by Detert and
393 Weitbrecht (2013).

394

395

396

397

398

399

400

401

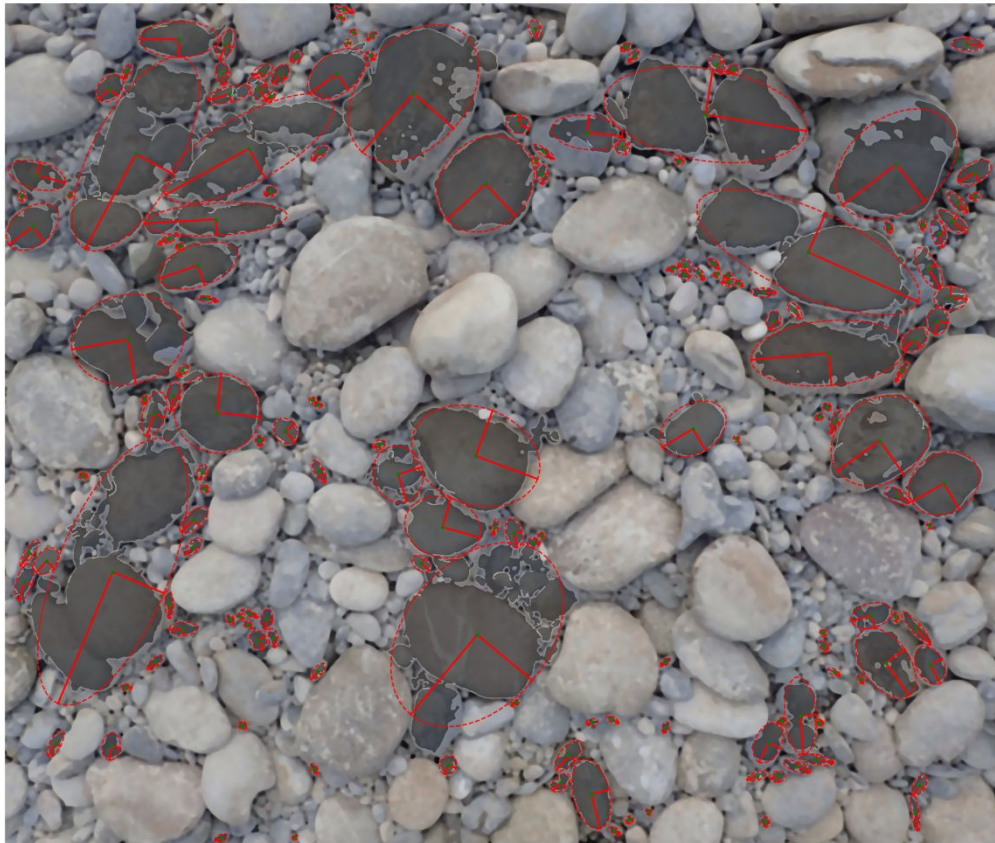


Fig. 4: Example of image processing by PebbleCounts software developed by Puriton & Bookhagen (2019).

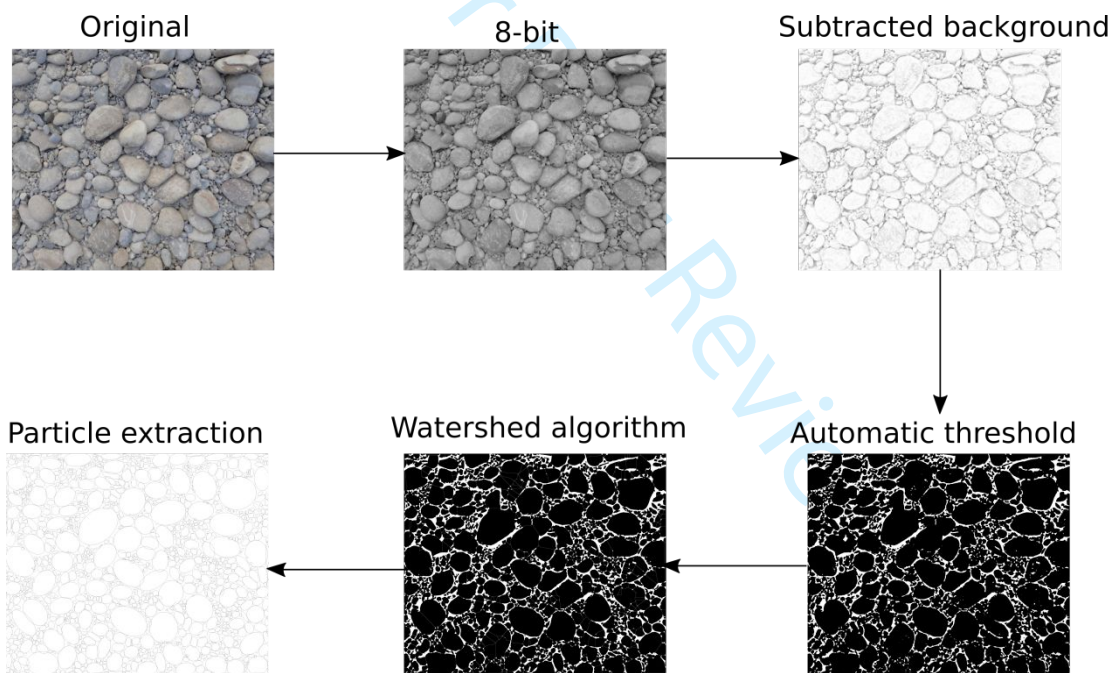


Fig. 5: Example of image processing by ImageJ software and based on the protocol developed by Sulaiman et al. (2014).

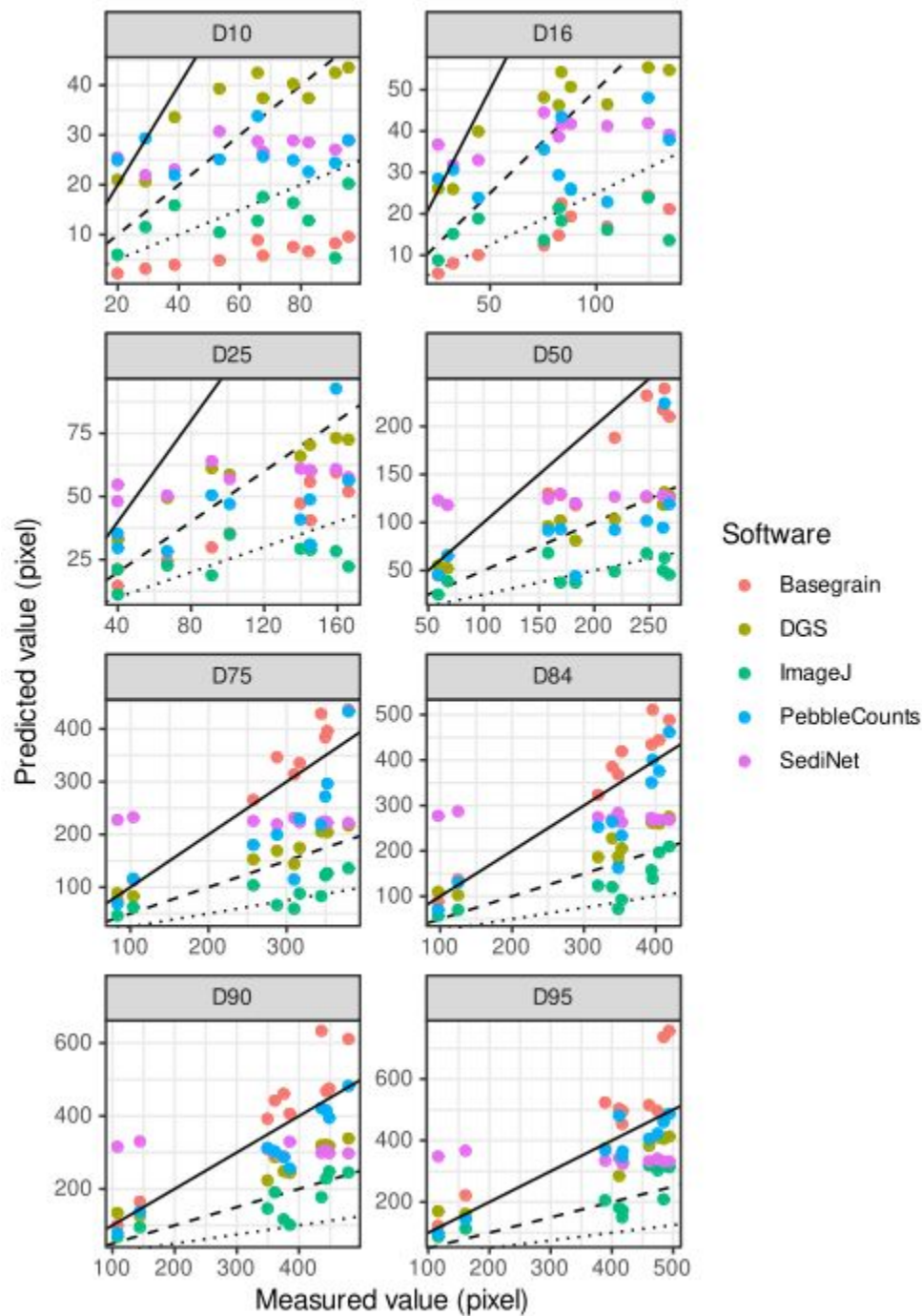


Fig. 6: Predicted percentiles of the GSD for the three methods according to manually measured percentiles before calibration. The black line and dotted black line correspond to the $y=x$ and $y = 1.5x$ line equations, respectively. Continuous black line, dashed black line and dotted black line corresponds to $y=x$ equation, $y=0.5x$ equation and $y=0.25x$ equation, respectively.

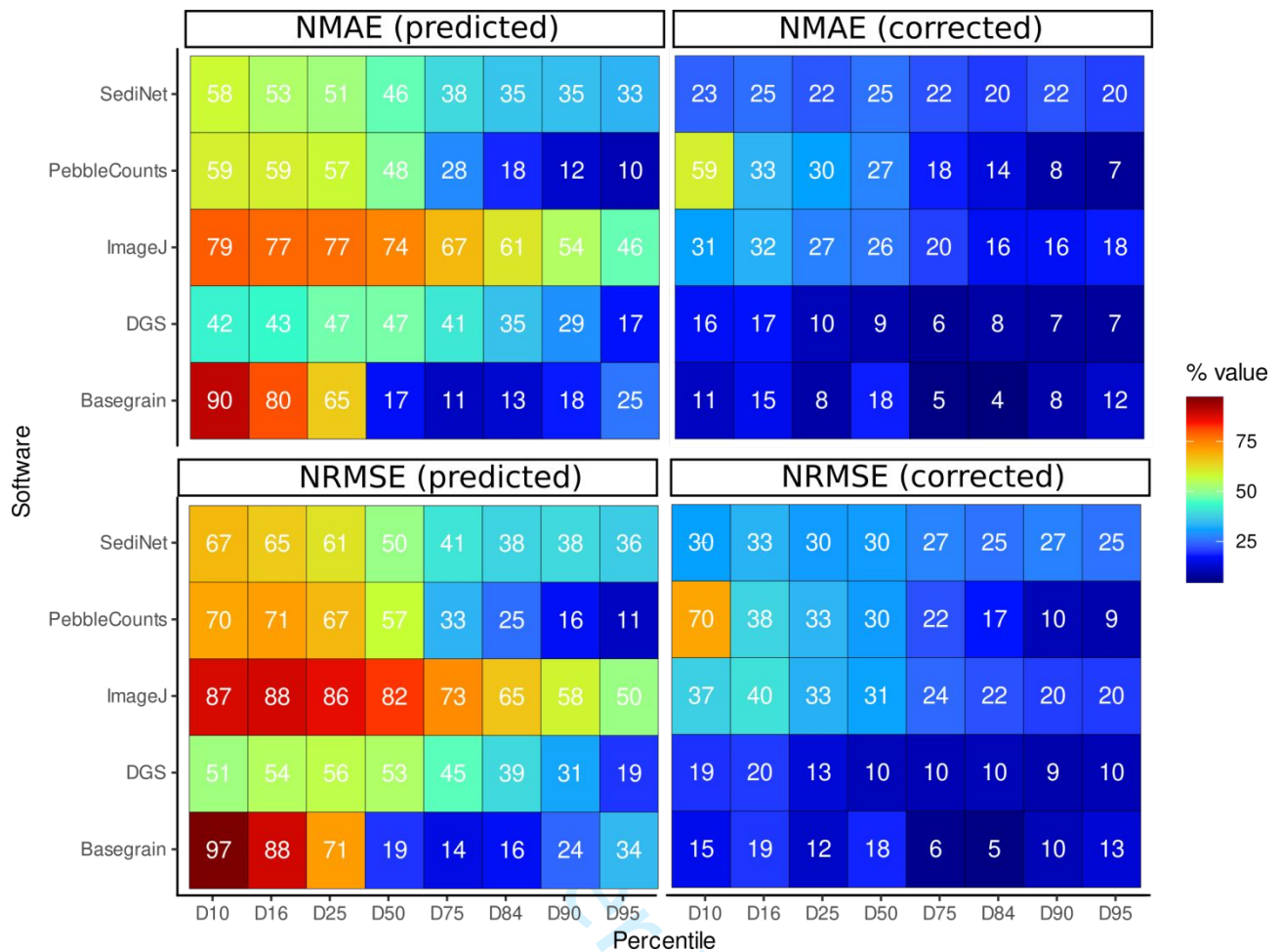


Fig. 7: Values of NRMSE (predicted and corrected) and NMAE (predicted and corrected) for each softwares. Predicted and corrected correspond respectively to no calibrated and calibrated results after linear regression application.

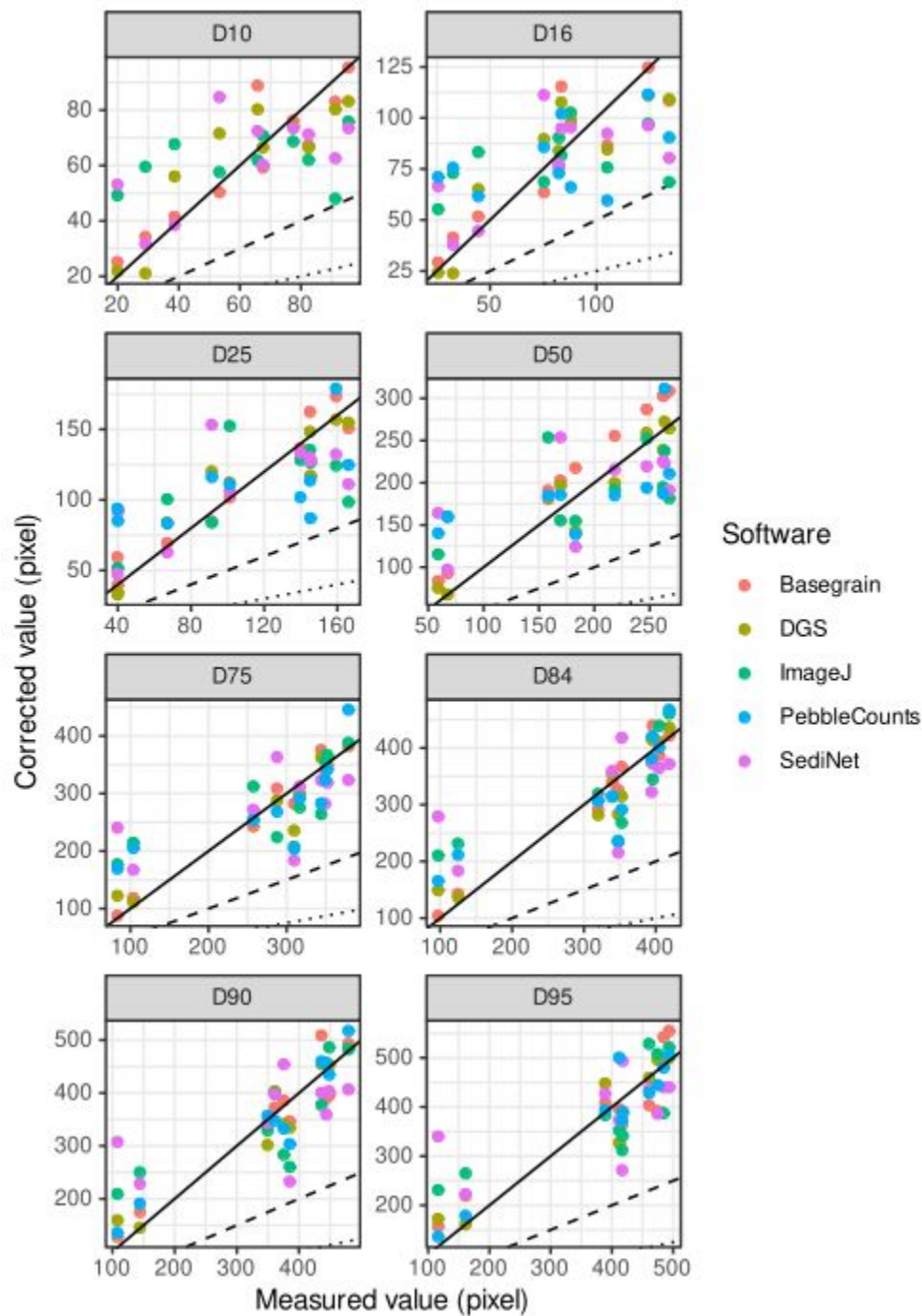


Fig. 8: Predicted percentiles of GSD for the three methods according to manually measured percentiles after calibration. Continuous black line, dashed black line and dotted black line corresponds to $y=x$ equation, $y=0.5x$ equation and $y=0.25x$ equation, respectively.

1
2 479
3
4
5
6
7
8
9
10
11
12
13
14
15
16
17
18
19
20
21
22
23
24
25
26
27
28
29
30
31 480
32
33
34 481
35
36
37 482
38
39
40 483
41
42
43
44
45
46

Percentile	DGS		Basegrain		ImageJ		PebbleCounts		SediNet	
	R ²	P-value	R ²	P-value	R ²	P-value	R ²	P-value	R ²	P-value
D ₁₀	0.76	0.00096	0.84	0.00018	0.12	0.33	0.04	0.31	0.41	0.047
D ₁₆	0.79	0.00065	0.80	0.00052	0.15	0.26	0.22	0.17	0.42	0.043
D ₂₅	0.89	4e-05	0.91	2.2e-05	0.37	0.061	0.35	0.075	0.48	0.026
D ₅₀	0.92	1e-05	0.94	3.7e-06	0.35	0.07	0.40	0.053	0.40	0.051
D ₇₅	0.92	1.4e-05	0.97	2.8e-07	0.51	0.02	0.59	0.0087	0.38	0.057
D ₈₄	0.90	2.4e-05	0.96	5.3e-07	0.57	0.011	0.72	0.0017	0.42	0.042
D ₉₀	0.92	9.4e-06	0.90	2.6e-05	0.64	0.0054	0.90	2.4e-07	0.36	0.063
D ₉₅	0.90	2.9e-05	0.84	0.00021	0.63	0.0065	0.92	1.4e-05	0.40	0.052

Tab. 1: R-square values of linear regressions and P-value between grain size percentiles estimated for each software according to grain size percentiles estimated manually.

Request for Changes to Journal Article Author List

What is this form for?

- Use this form to add or remove authors from an article.
- This form is not to request a post-publication change to an author's name (for example, to correct a misspelling). Please contact the Production Editor directly to make arrangements for these changes.
- This form is for use at all stages of submission and publication. **Change requests will not be considered unless the fully filled form is submitted.**

What should authors be aware of before completing and submitting this form?

- Requests to change an article's author list will be carefully reviewed by the Publisher and Editor, in line with the authors and contributors policies outlined in Wiley's [Best Practice Guidelines on Research Integrity and Publishing Ethics](#), by [Committee on Publication Ethics](#) guidance, and in the journal's Author Guidelines available on [Wiley Online Library](#).
- If your article has already been published, a change to the online Version of Record will require an enduring erratum/correction statement.
- The initiating author must provide to each involved party every page of this document, including this cover page, and any additional pages to be attached, for review.
- No co-author (those remaining, those newly added, those to be removed) or individuals and/or representatives of multi-author collaborative or consortia groups **should sign this form without reading** a) every page of this form in full including the cover page and any attachments, b) the relevant authorship and contributorship policies outlined on the cover page, and c) agreeing with all changes to the author list proposed herein.
- The Editor and Publisher are not empowered to arbitrate authorship disputes; in the event of an authorship dispute, consult your institution's research ethics department for guidance.

What will be required to complete this form?

- The undertaking—confirmed by way of a signature—of each and every involved party (those remaining, those newly added, those to be removed) that the requested change accurately reflects the authorship of the article at hand.
- A brief explanation of why the requested change is needed.

How do I submit this form and what will happen next?

- Submit the completed form to the journal's editorial or production office (visit the journal's homepage on [Wiley Online Library](#) to find the email address); incomplete forms will not be considered.
- Note that the below tables are in editable PDF format; we recommend completing the details using this functionality. If you are unable to use this functionality and require additional space, provide numbered attached documents with your request that clearly show the changes being requested.

- All authors (including any added or removed) should be copied on the email requesting the change.
- Wiley accepts handwritten signatures and e-signatures (e-signatures should preferably be provided using DocuSign, <https://go.docusign.com>; more information can be found at https://support.docusign.com/en/knowledgeSearch?by=topic&topic=sign_documents&category=sign). If authors are unable to sign on a single form, multiple versions of the same form, collated into a single PDF, will be acceptable.
- The Publisher and Editor may seek further information from each author on the requested change, if appropriate.
- The Publisher and Editor may seek further information from each author's institution on the requested change, if appropriate.

For Peer Review




Table 1. Article Information and change request

Article title	Comparison of software accuracy to estimate the bed grain size distribution from digital images: A test performed along
Journal title	River Research and Applications
Submission ID or DOI	RRA-21-0183.R1
Provide a brief explanation of and reason for the changes requested	One more co-author in the revised draft due to a scientific contribution

For Peer Review

No co-author (those remaining, those newly added, those to be removed) or individuals and/or representatives of multi-author collaborative or consortia groups **should sign this form without reading** a) every page of this form in full including the cover page and any attachments, b) the relevant authorship and contributorship policies outlined on the cover page, and c) agreeing with all changes to the author list proposed herein.

Table 2. Provide the complete and correct author list, in order, as it should appear on the article (attach an additional sheet if more space is needed)

Author Name**		Degree/s (e.g. BSc, PhD)	Corr. author (Y/N)	Institutional affiliation	Email address	ORCID iD or Scopus Author ID	Signature*	Date
Given Name†	Family Name							
Valentin	CHARDON	PhD	Y	CNRS, LIVE UMR 7362, U	valentin.chardon@li			27/09/202
Guillaume	PIASNY	BSc	N	CNRS, LIVE UMR 7362, U	guillaume.piasny@l			27/09/202
Laurent	SCHMITT	PhD	N	CNRS, LIVE UMR 7362, U	laurent.schmitt@un			27/09/202

*By signing Table 2, individuals and/or representatives of multi-author collaborative or consortia groups confirm that the author list shown here accurately reflect the authorship of the article cited in Table 1

†Include the author's middle initials with the given name, if applicable

**In cases of multi-author collaborative or consortia groups the most appropriate representative or legal guarantor must identify themselves and sign on behalf of the group

No co-author (those remaining, those newly added, those to be removed) or individuals and/or representatives of multi-author collaborative or consortia groups **should sign this form without reading** a) every page of this form in full including the cover page and any attachments, b) the relevant authorship and contributorship policies outlined on the cover page, and c) agreeing with all changes to the author list proposed herein.

Table 3. Provide the following information for each NEWLY ADDED author in Table 2 (leave blank if no new authors have been added)

Author Name**		Conflict of Interest statement	Acknowledgements	Contribution statement††
Given Name	Family Name			
Laurent	SCHMITT	none	none	writing, editing

**In cases of multi-author collaborative or consortia groups the most appropriate representative or legal guarantor must identify themselves and sign on behalf of the group

††Ensure the contribution statement aligns with the journal's contribution role taxonomy (e.g. CRediT), if relevant. This information can be found on the journal's Author Guidelines page on Wiley Online Library.

No co-author (those remaining, those newly added, those to be removed) or individuals and/or representatives of multi-author collaborative or consortia groups **should sign this form without reading** a) every page of this form in full including the cover page and any attachments, b) the relevant authorship and contributorship policies outlined on the cover page, and c) agreeing with all changes to the author list proposed herein.



Table 4. Provide a list of the individuals and/or representatives of multi-author collaborative or consortia groups to be REMOVED from the author list as it was originally provided for the article cited in Table 1 (leave blank if no authors are to be removed)

Author Name**		Institutional affiliation	Email address	Signature*	Date
Given Name†	Family Name				

*By signing Table 4, individuals and/or representatives of multi-author collaborative or consortia groups confirm that the author list shown in Table 2 accurately reflect the authorship of the article cited in Table 1
†Include the author's middle initials with the first name, if applicable
**In cases of multi-author collaborative or consortia groups the most appropriate representative or legal guarantor must identify themselves and sign on behalf of the group

For Peer Review

No co-author (those remaining, those newly added, those to be removed) or individuals and/or representatives of multi-author collaborative or consortia groups **should sign this form without reading** a) every page of this form in full including the cover page and any attachments, b) the relevant authorship and contributorship policies outlined on the cover page, and c) agreeing with all changes to the author list proposed herein.